

MambaIC: State Space Models for High-Performance Learned Image Compression

Fanhui Zeng^{1*}, Hao Tang², Yihua Shao³, Siyu Chen³, Ling Shao⁴, Yan Wang^{1†}

¹Institute for AI Industry Research (AIR), Tsinghua University

²School of Computer Science, Peking University

³University of Science and Technology Beijing

⁴UCAS-Terminus AI Lab, University of Chinese Academy of Sciences

Abstract

A high-performance image compression algorithm is crucial for real-time information transmission across numerous fields. Despite rapid progress in image compression, computational inefficiency and poor redundancy modeling still pose significant bottlenecks, limiting practical applications. Inspired by the effectiveness of state space models (SSMs) in capturing long-range dependencies, we leverage SSMs to address computational inefficiency in existing methods and improve image compression from multiple perspectives. In this paper, we integrate the advantages of SSMs for better efficiency-performance trade-off and propose an enhanced image compression approach through refined context modeling, which we term **MambaIC**. Specifically, we explore context modeling to adaptively refine the representation of hidden states. Additionally, we introduce window-based local attention into channel-spatial entropy modeling to reduce potential spatial redundancy during compression, thereby increasing efficiency. Comprehensive qualitative and quantitative results validate the effectiveness and efficiency of our approach, particularly for high-resolution image compression. Code is released at <https://github.com/AuroraZengfh/MambaIC>.

1. Introduction

Image compression is a crucial aspect of image storage and transmission, particularly in the era of high-definition, high-resolution, and large-scale digital images. In recent decades, traditional image formats such as JPEG [33], BPG [4], and VVC [5] have significantly advanced the digitalization process. With the rapid development of modern architectures like CNNs [20, 40], Transformers [9, 23], and others [32, 39], many learned image compression (LIC)

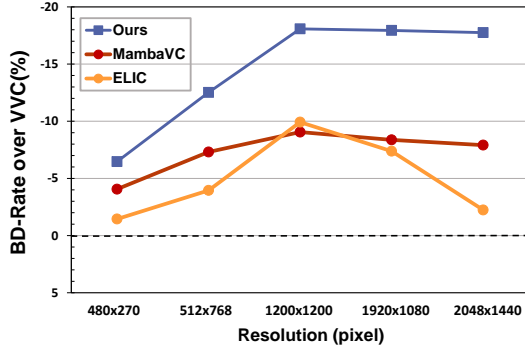


Figure 1. Performance of typical image compression approaches when resolution varies. Notably, our MambaIC consistently outperforms existing state-of-the-art methods [19, 35] and gets a more substantial improvement when the image scales up.

methods have emerged to achieve a better performance-efficiency trade-off. These methods typically consist of an encoder, decoder, and entropy model, and are optimized end-to-end. Recent works [19, 22, 26] even surpass the classical standards [5], demonstrating their potential to lead next-generation image compression standards and drive real-world applications in related industries.

Despite the rapid advancements achieved by pioneering works in both CNNs [3, 19] and Transformers [25, 34], limitations in performance and computational complexity hinder their practical applications. Specifically, while Transformer-based methods generally outperform CNN-based methods, they suffer from quadratic complexity proportional to pixel numbers, resulting in significant latency particularly for high-resolution image compression. Although efforts are made [22, 26] with well-designed modules to reduce computational load, the balance between performance and efficiency remains unsolved. This highlights the need for improving efficiency while maintaining high-performance in image compression.

In contrast to designing dedicated modules, another way

*Work done during internship at AIR, Tsinghua University

†Corresponding author. <wangyan@air.tsinghua.edu.cn>

to enhance LIC is to employ novel architectures. For example, introducing Transformer into LIC [34] brings significant improvements. Recent advances like State Space Models (SSMs) have demonstrated significant effectiveness, partly due to their reduced complexity and hardware-friendly computation. Therefore, various SSM variants have been applied to numerous downstream tasks [17, 44, 47]. As a novel paradigm, it offers inherent advantages over CNNs and transformers and paves a novel way for LIC. In terms of exploiting recent architectures for image compression, one concurrent work is MambaVC [35], which attempts to improve the efficiency of compression operations with an SSM structure. However, it merely replaces foundational blocks with SSM blocks without adjustments attached to the specific characteristics of SSM, resulting in sub-optimal performance compared to other well-designed image compression architectures.

In this work, we address two key challenges in image compression: *efficiency and performance*. To achieve these goals, we utilize SSMs to improve compression performance while enhancing computational efficiency, which can be validated by performance improvement of different resolutions illustrated in Figure 1. We employ SSMs into image compression framework and promote high-performance learned image compression from several perspectives. Specifically, we integrate SSMs into the context model to enrich the side information, thereby improving the efficiency and effectiveness of encoding and decoding. Additionally, we use channel-spatial entropy modeling with window-based local attention to better capture redundancy in latent representations, further boosting performance. We conduct extensive experiments, and the results demonstrate that the proposed method is both effective and efficient. Notably, MambaIC shows excellent efficiency in high-resolution image compression. Comprehensive analysis and visualization further certify its usefulness.

Our contributions can be summarized as follows:

- To the best of our knowledge, we are the first to integrate SSMs into both nonlinear transform and context model for high-performance learned image compression.
- We incorporate window-based local attention into channel-spatial entropy modeling to reduce spatial redundancy as well as enhancing the compression pipeline.
- We conduct comprehensive experiments and analyses to demonstrate that the proposed method is effective, efficient with superior qualitative and quantitative results, particularly for high-resolution images.

2. Related Work

2.1. State Space Models

State Space Models (SSMs) [14, 29] is becoming an emerging and promising direction for modern architecture appli-

cations. It aims to tackle the problem of computational efficiency in modeling long-range dependencies [10, 42] from a novel perspective and seeks to process long sequences with linear-time complexity. Following the pioneering structured state-space model (S4) [15], numerous works [12, 38] improve the performance.

As a notable milestone, Mamba [8, 13] introduces an input-dependent selection technique into S4 and largely enhances SSM with a novel structure. Due to its impressive potential, many efforts have been paid to promote the scanning mechanism to refine long-range modeling in vision tasks [17, 21, 27, 47]. Specifically, Vim [27] incorporates bidirectional sequence modeling with positional awareness for visual understanding. Mambavision [17] proposes a redesigned, vision-friendly, hybrid Mamba block to enhance global context learning. LocalMamba [21] introduces a local scan with distinct windows to enhance visual representations. The success of SSMs has also inspired widespread application in various downstream tasks of the vision domain [11, 16, 37, 44]. In this work, our aim is to specifically design the structure of SSMs to leverage the power for image compression.

2.2. Learned Image Compression

Compression [36, 43, 46] plays a vital role in acceleration and learned image compression [31] targets optimizing rate-distortion trade-off exploiting neural networks as image compression operator. Modern learned image compression framework fundamentally constructs upon entropy model [2], followed by employing hyperprior [3] to calculate the entropy parameters and many specific structural improvements [6, 7, 49].

With the widespread adoption of Transformer [10, 42], they are also used in image compression [28]. However, computational efficiency remains a critical problem due to the quadratic growth time complexity despite the remarkable progress in performance and many works seek to tackle the problem with fine architecture design [19, 22, 26]. As a concurrent exploration, MambaVC [35] first attempts to build a compression framework based on SSM [13]. However, it employs mamba blocks without special adaptation, leading to inferior performance. In this paper, we comprehensively analyze the characteristics of SSMs in compression and enhance image compression with better rate-distortion performance.

2.3. Context Models

Many works have focused on reducing bitstream with context model. Minnen et al. [31] proposes to estimate current representations using previously coded ones for better compression performance. Moreover, with impressive progress accomplished by channel-wise and checkerboard auto-regressive models [18, 19, 30] that split the represen-

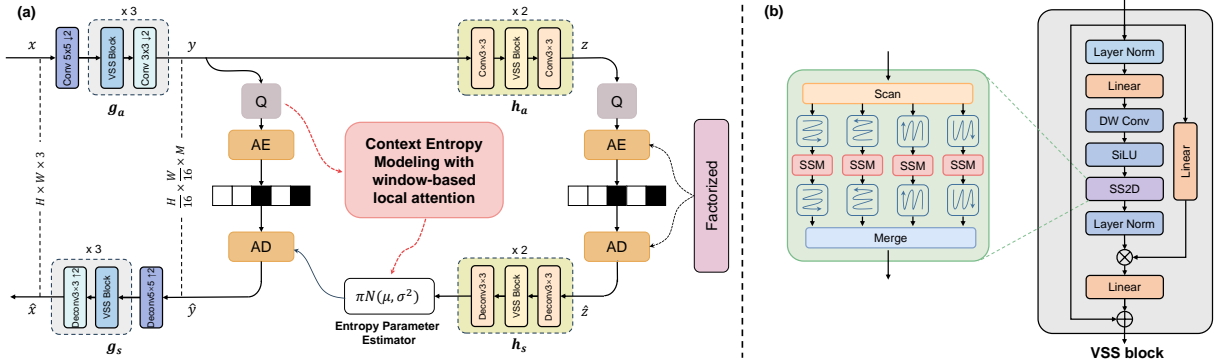


Figure 2. (a) Overall architecture of the proposed method. AE and AD are arithmetic encoder/decoder with residual bottleneck blocks. The proposed context entropy model consists of channel-spatial context model and window-based local attention to estimate entropy parameters. (b) Structure of visual state space (VSS) block with 2D selective scan.

tation into groups and encode each group conditioned on coded symbols of previous groups, some progress with respect to Transformer [25, 34, 48] also gains promotion.

Despite the achievements, computational complexity still remains a challenge for existing approaches. For the first time, we explore an efficient context model that incorporates SSMs for learned image compression to achieve competitive results against existing CNN/transformer methods with better computational efficiency.

3. The Proposed Method

We begin with problem formulation and notation for clear statement in Section 3.1. Then we describe the proposed method termed MambaIC in Section 3.2, which is composed of SSM-based nonlinear transform, context model, and window-based local attention for channel-spatial entropy modeling in an attempt to improve computational efficiency and enhance effectiveness. The overall pipeline and detailed module structure are shown in Figure 2.

3.1. Problem Formulation and Notations

Learned image compression. Typically, a given input image x is first encoded into latent representation y through neural analyzer g_a parametered by θ_{g_a} :

$$\mathbf{y} = g_a(\mathbf{x}; \boldsymbol{\theta}_{q_a}). \quad (1)$$

Hyper prior encoder/decoder h_a and h_s are employed to learn the mean and variance of latent features by hyperprior representation z extracted from y :

$$\begin{aligned} z &= h_a(\mathbf{y}; \boldsymbol{\theta}_{h_a}), \\ \mu, \sigma^2 &= h_s(\hat{\mathbf{z}}, \boldsymbol{\theta}_{h_s}). \end{aligned} \tag{2}$$

The discrete coding-symbols \hat{y} and \hat{z} are obtained from quantized latent and hyperprior representations:

$$\begin{aligned}\hat{\mathbf{y}} &= \mathcal{Q}(\mathbf{y} - \boldsymbol{\mu}) + \boldsymbol{\mu}, \\ \hat{\mathbf{z}} &= \mathcal{O}(\mathbf{z}),\end{aligned}\tag{3}$$

where $Q(\cdot)$ stands for quantization operator, and entropy model is formulated as conditioned gaussian form to estimate the conditional distribution of latent representation:

$$p_{\hat{\mathbf{y}}|\hat{\mathbf{z}}}(\hat{\mathbf{y}}|\hat{\mathbf{z}}) = [\mathcal{N}(\boldsymbol{\mu}, \boldsymbol{\sigma}^2) * U(-0.5, 0.5))](\hat{\mathbf{y}}), \quad (4)$$

and \hat{x} is the reconstructed images in pixel space from neural synthesizer g_s parametered by θ_{g_s} :

$$\hat{\mathbf{x}} = g_s(\hat{\mathbf{y}}, \theta_{g_s}). \quad (5)$$

During training, lagrangian multiplier λ is introduced to adjust the rate-distortion optimization and control bit rate in an end-to-end manner:

$$\mathcal{L} = \lambda \mathcal{D}(\mathbf{x}, \hat{\mathbf{x}}) + \mathcal{R}(\hat{\mathbf{y}}) + \mathcal{R}(\hat{\mathbf{z}}), \quad (6)$$

where $\mathcal{D}(\mathbf{x}, \hat{\mathbf{x}})$ measures the distortion by mean squared error (MSE) and $\mathcal{R}(\hat{\mathbf{y}})$, $\mathcal{R}(\hat{\mathbf{z}})$ are bit rates of $\hat{\mathbf{y}}$ and $\hat{\mathbf{z}}$ estimated by entropy model.

State space models. SSMs [15] can be viewed as linear time-invariant (LTI) systems. Dynamic response $y(t) \in \mathbb{R}^L$ is stimulated from input $x(t) \in \mathbb{R}^L$ through intermediate hidden state $h(t) \in \mathbb{R}^N$, which can be described in the form of linear ordinary differential equations (ODEs):

$$\begin{aligned} \mathbf{h}'(t) &= \mathbf{A}\mathbf{h}(t) + \mathbf{B}\mathbf{x}(t), \\ \mathbf{y}(t) &= \mathbf{C}\mathbf{h}(t), \end{aligned} \quad (7)$$

where $\mathbf{A} \in \mathbb{R}^{N \times N}$, $\mathbf{B} \in \mathbb{R}^{N \times 1}$, $\mathbf{C} \in \mathbb{R}^{N \times 1}$ are state transition matrices, respectively. Under the zero-order hold assumption that the value of input x is constant over the interval Δ , The parameters of continuous system can be discretized into the following form:

$$\begin{aligned}\bar{\mathbf{A}} &= \exp(\Delta \mathbf{A}), \\ \bar{\mathbf{B}} &= (\Delta \mathbf{A})^{-1}(\exp(\Delta \mathbf{A}) - \mathbf{I}) \cdot \Delta \mathbf{B}.\end{aligned}\quad (8)$$

Consequently, the discrete equation of Eq. (7) can be reformulated as:

$$\begin{aligned} \mathbf{h}_t &= \bar{\mathbf{A}}\mathbf{h}_{t-1} + \bar{\mathbf{B}}\mathbf{x}_t, \\ \mathbf{y}_t &= \mathbf{C}\mathbf{h}_t. \end{aligned} \tag{9}$$

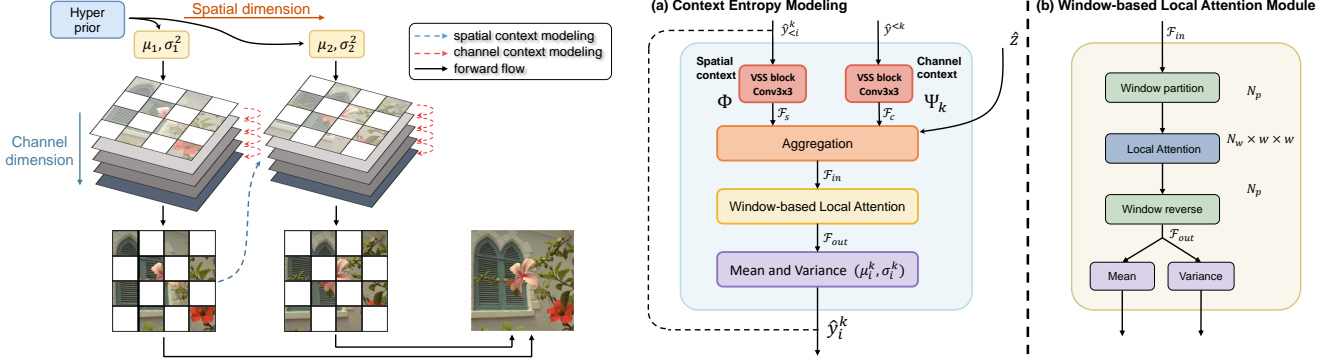


Figure 3. *Left:* Illustration of hybrid context modeling. Hyperprior together with symbols of previous channels estimates the parameters of anchors, which are used by the prediction of non-anchors spatially. Both anchors and non-anchors are integrated to generate the entire latent representations. *Right:* Detailed procedure of (a) auto-regressive context entropy modeling with (b) window-based local attention.

Subsequently, a global convolution is incorporated for parallel computation.

Context model with hybrid auto-regression. To enhance the entropy model and mitigate redundancy, context learning [31] separates the spatial information and recovers the features in an auto-regressive convolution. For latent representations \hat{y}_i , context model refers to neighbours with spatial relation:

$$\hat{y}_i = \Phi(\hat{y}_{<i}; \theta), \quad (10)$$

where Φ is used to estimate the entropy parameters with hyperprior \hat{z} . As an improvement, checkerboard [18] groups them into anchors and non-anchors and therefore replace the auto-regressive decoding into masked latent modeling, which significantly accelerates the process.

In addition to spatial context modeling, channel-wise auto-regressive modeling [30] further splits the channels into K chunks, and predicts the symbols on context of previous channels to enhance dimensional expression:

$$\hat{y}^k = \Psi_k(\hat{y}^{<k}, \theta_k), \quad k = 2, \dots, K, \quad (11)$$

where Ψ_k is entropy parameter estimator of the k^{th} chunk along channel dimension.

Built upon this, ELIC [19] further integrates both checkerboard and channel-wise autoregressive modeling, and the resultant hybrid context model is illustrated in left of Figure 3. In this paper, we also combine both advantages and exploit channel-spatial context model with uniform chunks along dimension.

3.2. Overall Architecture of MambaIC

Due to the efficiency of SSM shown in previous research [13, 47], we employ it as the foundation component and explore better mechanisms tailored for the adaptation in image compression. Generally, we employ 2D selective scan as the foundation block in nonlinear transform and context model to predict the mean μ and the variance σ of

the Gaussian entropy model [31] and decode latent representations with fine window-based local attention through arithmetic decoder (AD). The overall structure of the proposed method is shown in Figure 2a.

SSM-based contextual model. For SSM block, we utilize visual state space (VSS) [17, 47] block in parameter estimator for context modeling. As shown in Figure 2b, visual state space block consists of a composition of layer normalization, linear layer, depthwise convolution (DW Conv), SiLU activation and the core 2D selective scan (SS2D). Concretely, SS2D first scans the input patches along four distinct traversal paths, applies a separate SSM block to process each patch, and then merges them back to 2D output. Through cross-scanning and merging, SS2D effectively integrates information from all relevant pixels in 2D space and enhances global receptive fields, which greatly enhances image compression with advanced representation.

We integrate visual state space block in contextual entropy modeling Ψ_k and Φ for compact and effective bit-stream representation in the channel-spatial direction as shown in Figure 3a. Explicitly, for decoding of the symbol at i^{th} location of the k^{th} chunks, Ψ_k and Φ are incorporated for modeling the channel context $\hat{y}^{<k}$ and spatial context $\hat{y}_{<i}^k$, respectively. Ψ_k and Φ consist of convolution block and VSS block to enrich channel-spatial context information, which can be formulated as:

$$\begin{aligned} \mathcal{F}_c &= \Psi_k(\hat{y}^{<k}) = \text{Conv}(\text{VSS}(\hat{y}^{<k})), \\ \mathcal{F}_s &= \Phi(\hat{y}_{<i}^k) = \text{Conv}(\text{VSS}(\hat{y}_{<i}^k)), \end{aligned} \quad (12)$$

where \mathcal{F}_c and \mathcal{F}_s represents channel and spatial features, respectively. Compact latent representations with rich information are therefore obtained with estimated parameters from parameter aggregation effectively.

The \hat{y}^k is then used to calculate the features of the next decoded symbol through the spatial/channel context modeling in the circle. Finally, all chunks of \hat{y}^k are concatenated, and obtain the decoded latent representation \hat{y} .

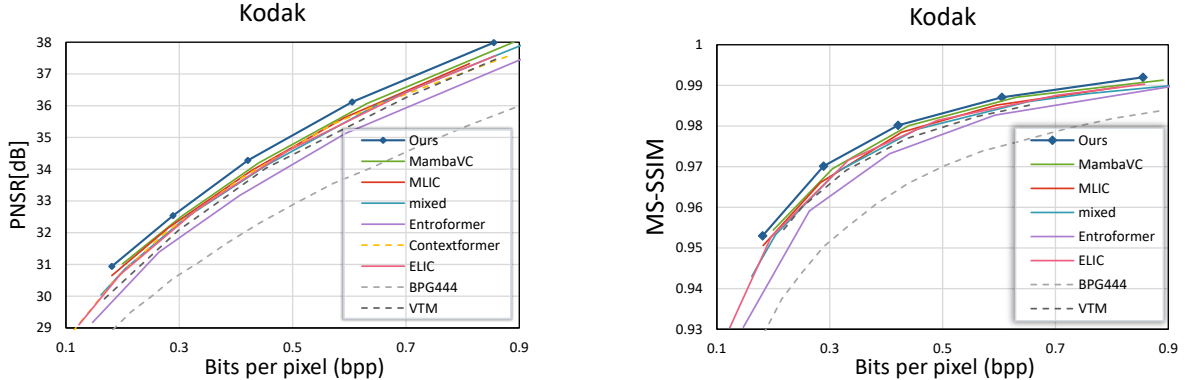


Figure 4. Results on Kodak. Performance is measured with PSNR and MS-SSIM. Left-top represents better performance. We compare with numerous learned compression methods as well as conventional coding like BPG and VTM. Zoom in for a better view.

In practical implementation, we use a parallel checkerboard mask model [18] for spatial context modeling, which means the latent representations are grouped into anchors and non-anchors. The context prior to $\hat{y}_{<i}^k$ is \emptyset for *anchors* and anchors for *non-anchors*, respectively.

Window-based local attention for auto-regressive modeling. Proper entropy modeling and latent representation are vital for effective information compression. As SSM block effectively captures global receptive fields, we additionally perform local attention in context entropy modeling. As illustrated in Figure 3b, we incorporate window-based local attention (WLA) following latent parameter aggregation. Specifically, WLA consists of window partition \mathcal{W}_p that splits patches N_p into smaller window size N_w , local attention (\mathcal{WA}) operating on $N_w \times w \times w$) that efficiently models local relation within windows and window reverse \mathcal{W}_r to recover the representation formulated as:

$$\mathcal{F}_{out} = \mathcal{W}_r(\mathcal{LA}(\mathcal{W}_p(\mathcal{F}_{in}))). \quad (13)$$

The window-based local attention has two advantages: (1) improve efficiency with attention on fewer patches; (2) enhance local relation description for better redundancy mitigation since visual state space block builds upon getting global receptive fields. Therefore, we are capable of facilitating both effectiveness and efficiency in the SSM-based image compression paradigm.

Formally, mean and variance for entropy modeling in each context model is formulated as:

$$(\mu_i^k, \sigma_i^k) = \text{WLA}(\text{ParamAgg}(\mathcal{F}_c, \mathcal{F}_s, h_s(\hat{z}))), \quad (14)$$

where $\text{WLA}(\cdot)$ is window-based local attention. The estimated entropy parameters are then separately utilized for Gaussian entropy modeling of latent representations.

4. Experiments

4.1. Setups

Baselines. We undertake a comparison of our approach with multiple existing state-of-the-art image compres-

sion techniques for both CNN/Transformer-based methods including ELIC [19], Mixed [26], MLIC [22], Entroformer [34], Contextformer [25] and MambaVC [35]. Also, we include conventional coding methods BPG [4] and VTM [5] for a comprehensive comparison.

Datasets. For performance evaluation, we employ Kodak [24], Tecnick [1] and CLIC Professional Valid [41] as validation datasets for exhaustive evaluation. PSNR and MS-SSIM are used to comprehensively measure the distortion of the reconstructed images, and bits per pixel (bpp) is used to measure compression ratio (PSNR is expressed in logarithmic decibel units). For training, we use Flickr30k [45] which is composed of 31783 images. More details are shown in Appendix A and B.

4.2. Implementation Details

The model is optimized with mean square error (MSE) loss and we use a $\lambda \in \{0.0035, 0.0067, 0.013, 0.025, 0.05\}$ as the multiplier for different bitrates. We train the model for 250 epochs. The number of channels N for \mathbf{z} is 128. Number of channel M for \mathbf{y} is 320 and we set number of channel chunks K to be 5. More implementation details are exhibited in Appendix C.

4.3. Rate-Distortion Performance

Comparison on common datasets. We present the comparison with existing methods on commonly evaluated datasets in Figure 4. It is illustrated that our method achieves the best rate-distortion trade-off in both PSNR and MS-SSIM and consistently outperforms previous methods by a substantial margin, firmly verifying the effectiveness of our approach. Notably, compared to MambaVC with similar SSM structure, our method receives obvious improvements, showcasing that the proposed MambaIC is capable of obtaining high performance against Transformer, CNN, and conventional coding algorithms while integrating the advantage of SSMs for image compression at the same time. **Scaling to higher resolution.** Due to the surge in demand

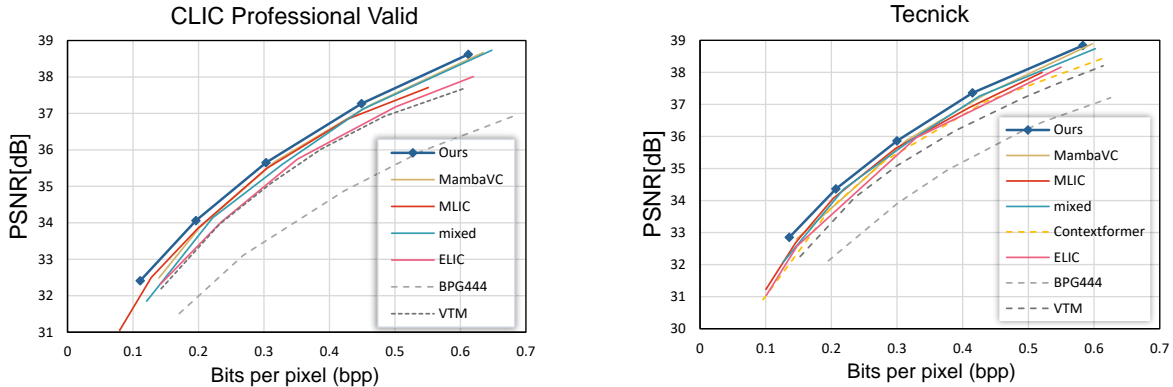


Figure 5. Performance on datasets with higher resolution including Tecnick and CLIC professional valid measured with PSNR. Left-top indicates better performance. Our method gets a consistent improvement when images scale up. Zoom in for a better view.

for higher image sharpness, compression efficiency for images of higher resolution has received a large amount of attention. The primary advantage of SSMs is their effective computation, while maintaining global receptive fields. It is shown in Figure 5 that when the validation dataset varies to higher resolution (1200×1200 for Tecnick and 2048×1440 for CLIC Professional Valid), our approach remains stable and gets competitive results against previous methods, strongly confirming the effectiveness and stability of the method. The conclusion is further confirmed in Figure 1, in which we present the BD-rate curve when the resolution of compressed images varies. It is shown that our method gets consistent improvements against existing methods. Specifically, the promotion becomes more substantial when the image scales up, where the performance of existing approaches shows varying degrees of degradation, whereas our method remains stable. It is of great significance in vast, high-definition, and large-scale image transmission in the era of big data.

BD-rate comparison. To have a quantitative comparison of the mentioned methods, we report BD-rate results anchored on the manually designed VVC image codec across different datasets. Table 1 reveals that our approach outperforms conventional standard on RD performance regarding PSNR, and also surpasses existing methods by a substantial margin. Specifically, compared with typical context model in both CNN and transformer, our method gets impressive gains (8.57% and 7.47%, respectively). Also, in comparison to SSM-based model MambaVC [35], considerable 5.21% improvement strongly certifies the effectiveness of our method for high-performance image compression.

4.4. Efficiency Analysis

To further substantiate the efficiency of MambaIC, we compare it with various existing methods and systematically analyze the efficiency of the proposed method from the perspective of inference latency.

Table 1. RD performance and complexity comparison of learned image compression evaluated on Kodak. Results marked with \dagger are from the original paper due to the absence of code. Typical CNN/Transformer methods are selected for comparative analysis. Arithmetic decoding time is included in decoding latency.

Method	Inference Latency (ms)		FLOPS (/G)	BD-Rate
	Enc.	Dec.		
VVC [5]	-	-	-	0.00
ELIC [19]	40.76	45.34	109.38	-3.95%
Contextformer \dagger [25]	40.00	44.00	-	-5.05%
MambaVC [35]	60.45	41.67	135.64	-7.31%
Mixed [26]	127.36	91.44	211.54	-7.39%
Ours	60.73	39.42	202.04	-12.52%

Inference latency. With the increasing demand for real-time transmission, the speed of inference, especially the decoding time, greatly determines the utility of the actual scenario applications. In Table 1, we compare the inference efficiency, *e.g.*, encoding and decoding time of different approaches. Concretely, due to the well-designed context model with window-based local attention for entropy modeling and latent representation decoding, MambaIC achieves higher performance, *e.g.*, BD-rate, and lower decoding latency without sacrificing the speed of encoding. It is worth highlighting that compared to state-of-the-art mixed transformer-CNN architectures [26], MambaIC achieves notable **2.87%** higher BD-rate with around **50%** of encoding time and **30%** of decoding time, firmly demonstrating the efficacy and efficiency of the proposed method.

4.5. Ablation Study

We comprehensively analyze the influence of different structures and hyper-parameters in the proposed framework. More results can be found in Appendix D.

Impact of each component. We study the effectiveness of each component proposed for enhancing image compression with SSMs and showcase the results in Table 2. It is

Table 2. Ablation study of each component in MambaIC. Results are evaluated on Kodak. BD-rate is compared to VVC. CAM and WLA refers to channel-wise auto-regressive modeling and window-based local attention, respectively.

Method	Inference Latency (ms)		BD-Rate
	Enc.	Dec.	
VVC [5]	-	-	0.00
w/o CAM	23.41	16.72	-6.73%
w/o spatial context model	46.51	32.73	-8.54
w/o WLA	58.40	35.14	-9.17%
Ours	60.73	39.42%	-12.52%

Table 3. Effectiveness of SSM block in the model. We implement two variants that replace SSM with CNN/Transformer.

Foundation Blocks	Decoding Latency (ms)	BD-rate
CNN	35.53	-3.81%
Transformer	48.74	-7.19%
State Space Model (Ours)	39.42	-12.52%

elucidated that each designed component of our approach are of great significance to high-performance image compression. Specifically, all added modules do not bring significant delay increases and play a vital role in improving compression performance (5.79%, 3.98% and 3.35%, respectively). Moreover, compared to CAM that adds 22.70 ms latency, the proposed context model and window-based local attention only result in relatively small decoding latency (6.69 and 4.28 ms, respectively), which can be attributed to the efficiency of compact latent representation and SSM block in the proposed framework. Finally, integrating all of them, *i.e.*, MambaIC achieves the best results, substantiating that the proposed context modeling techniques tailored for SSMs contribute fundamentally to the enhancement of latent representation coding and thus achieve high-performance image compression.

Effectiveness of SSM block. The composition of SSM block in compression model is of vital importance to enhancing the performance of image compression. To validate the utility of SSM block in boosting rate-distortion performance, we implement two variants that replace the foundation blocks of MambaIC from SSM block to CNN and transformer, respectively. As shown in Table 3, our method with SSM block achieves substantial improvements against the two variants regarding rate-distortion balance, *i.e.*, BD-rate, showcasing the utility of the proposed techniques tailored for enhancing performance of SSM blocks. In terms of efficiency, CNN exceeds all, closely followed by SSM, with the transformer exhibiting the lowest efficiency. The outcome certifies that, considering both, the

Table 4. Bitstream comparison of different methods with PSNR approximately 34.2 dB on Kodak. Previous methods are either equipped solely with local or global receptive fields. Our method benefits from local attention for performance enhancement.

Method	Receptive fields	Window size	Bpp	Δ Bpp (%)
ELIC [19]	local	-	0.4683	-
Contextformer [25]	global	-	0.4596	1.86%
MambaVC [35]	global	-	0.4482	4.29%
Ours	global	6×6	0.4428	5.44%
	+	8×8	0.4404	5.95%
	local	10×10	0.4417	5.68%

SSM block achieves a better balance between efficiency and performance and has the potential to become a foundation block in image compression.

Influence of local window size. Window-based local attention is of crucial significance in mitigating the spatial redundancy and obtaining compact bitstream representation. It is shown in Table 4 that first, previous methods possess global or local receptive fields, leading to insufficient and inefficient bitstream coding. By contrast, our approach enhances the global receptive fields of SSMs with window-based local attention, which significantly contributes to compact bitstream representation (5.95% bitstream saving). Moreover, window size has a moderate influence on the performance. Considering that a larger window size may not obtain information with compact local relation and a smaller window size may have a negative impact on the balance between global receptive field and local redundancy elimination, we select the window size to be 8×8 in the main experiments.

4.6. Qualitative Analysis

In addition to quantitative experiments, we provide further qualitative results to intuitively demonstrate the effectiveness of the proposed method.

MambaIC achieves high quality decompression performance. To showcase deeper analysis of the proposed MambaIC, we visualize a few compressed images after decoding and present qualitative results in Figure 6 to have a better understanding of the performance. Intuitively, compared to existing methods, MambaIC shows obvious high-quality decompression performance with fine local features and edge details. Specifically, compared to BPG and ELIC, our image demonstrates a superior restoration effect of the sculpted chin and clothes, making them more realistic (left of Figure 6). Additionally, it offers improved consistency and a more detailed depiction of the parrot’s hair and body edges (right of Figure 6). The outcomes strongly certificate that MambaIC is capable of guaranteeing high-performance image compression.

MambaIC effectively reduces redundancy with context



Figure 6. Visualization of decompressed images *kodim17.png* and *kodim23.png* in Kodak using different compression strategies. The local details are enlarged to better highlight the difference. Zoom in for a better view.

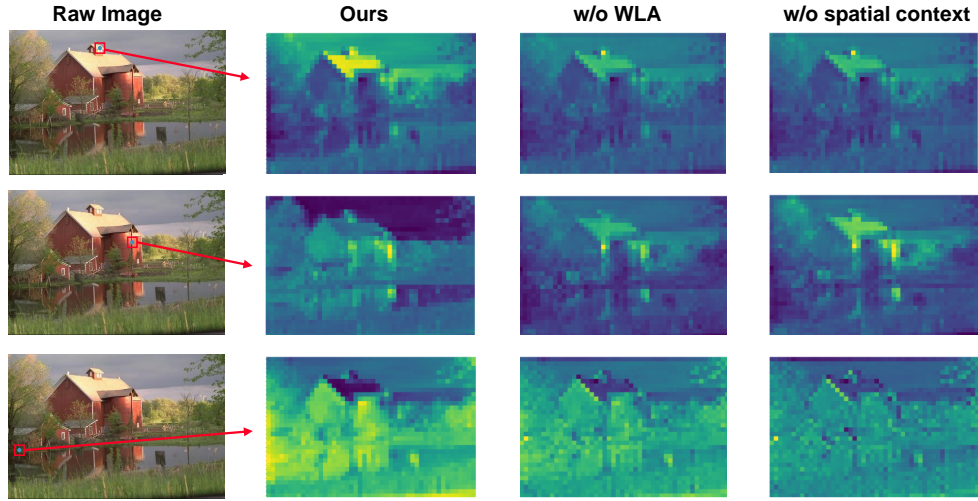


Figure 7. Attention maps of latent representations y of *kodim22.png* in Kodak focusing on typical points spatially. WLA represents the proposed window-based local attention. Equipped with context entropy modeling and window-based local attention, key points of MambaIC focus on regions with strong spatial relation and therefore the method achieves compact and high-performance latent representation.

modeling and fine local attention. As stated in Section 3.2, both context modeling and window-based local attention tailored for SSM-based image compression are of great significance for spatial relation description as well as high performance. We also visualize the attention map of the images decompressed by different methods and focus on several key points in Figure 7. It can be seen that no matter which points the models pay attention to, our method always better captures exact local regions, *i.e.*, the roof (*top*), the main body of the house (*middle*), and trees and reflections in the lake (*bottom*), with similar and strong-correlated content information. For example, our method precisely and effectively enhances attention on the house (the second row), while contrast methods focus their attention on the sky. In the third row, MambaIC accurately identify regions with strong correlated, while contrast methods present a wide and divergent attention to the entire image. It is illustrated that, unlike an approach without window attention, MambaIC better helps focus on crucial spatial points and therefore eliminate redundancy as much as possible. Moreover, context modeling contributes to latent representation with rich side information, thereby enhancing compact local

relations. All visualizations vividly certificate the utility of the proposed method for compact latent representation and therefore achieving high-performance image compression.

5. Conclusion

In this paper, we explore SSM for high-performance learned image compression and introduce MambaIC to tackle the problem of *computational efficiency* and *effectiveness*. In particular, we introduce context modeling into SSM-based compression pipeline, which empowers entropy modeling with rich side information. Then an efficient window-based local attention is employed to eliminate spatial redundancy. Both qualitative and quantitative experimental results certificate the effectiveness against existing methods with superior efficiency, and the improvement is especially substantial with higher resolution.

Acknowledgements

This work is supported by Wuxi Research Institute of Applied Technologies, Tsinghua University under Grant 20242001120, and the Fundamental Research Funds for the Central Universities, Peking University.

References

[1] Nicola Asuni, Andrea Giachetti, et al. Testimages: a large-scale archive for testing visual devices and basic image processing algorithms. In *STAG*, pages 63–70, 2014. 5

[2] Johannes Ballé, Valero Laparra, and Eero P Simoncelli. End-to-end optimized image compression. In *5th International Conference on Learning Representations, ICLR*, 2017. 2

[3] Johannes Ballé, David Minnen, Saurabh Singh, Sung Jin Hwang, and Nick Johnston. Variational image compression with a scale hyperprior. In *International Conference on Learning Representations*, 2018. 1, 2

[4] Fabrice Bellard. Bpg image format. <https://bellard.org/bpg>, 2015. 1, 5

[5] Benjamin Bross, Ye-Kui Wang, Yan Ye, Shan Liu, Jianle Chen, Gary J Sullivan, and Jens-Rainer Ohm. Overview of the versatile video coding (vvc) standard and its applications. *IEEE Transactions on Circuits and Systems for Video Technology*, 31(10):3736–3764, 2021. 1, 5, 6, 7

[6] Fangdong Chen, Yumeng Xu, and Li Wang. Two-stage octave residual network for end-to-end image compression. In *Proceedings of the AAAI Conference on Artificial Intelligence*, pages 3922–3929, 2022. 2

[7] Zhengxue Cheng, Heming Sun, Masaru Takeuchi, and Jiro Katto. Learned image compression with discretized gaussian mixture likelihoods and attention modules. In *Proceedings of the IEEE/CVF conference on computer vision and pattern recognition*, pages 7939–7948, 2020. 2

[8] Tri Dao and Albert Gu. Transformers are ssms: Generalized models and efficient algorithms through structured state space duality. In *Forty-first International Conference on Machine Learning*, 2024. 2

[9] Alexey Dosovitskiy. An image is worth 16x16 words: Transformers for image recognition at scale. *arXiv preprint arXiv:2010.11929*, 2020. 1

[10] Alexey Dosovitskiy, Lucas Beyer, Alexander Kolesnikov, Dirk Weissenborn, Xiaohua Zhai, Thomas Unterthiner, Mostafa Dehghani, Matthias Minderer, Georg Heigold, Sylvain Gelly, et al. An image is worth 16x16 words: Transformers for image recognition at scale. In *International Conference on Learning Representations*, 2021. 2

[11] Zhengcong Fei, Mingyuan Fan, Changqian Yu, Debang Li, Youqiang Zhang, and Junshi Huang. Dimba: Transformer-mamba diffusion models. *arXiv preprint arXiv:2406.01159*, 2024. 2

[12] Daniel Y Fu, Tri Dao, Khaled Kamal Saab, Armin W Thomas, Atri Rudra, and Christopher Re. Hungry hungry hippos: Towards language modeling with state space models. In *The Eleventh International Conference on Learning Representations*, 2022. 2

[13] Albert Gu and Tri Dao. Mamba: Linear-time sequence modeling with selective state spaces. *arXiv preprint arXiv:2312.00752*, 2023. 2, 4

[14] Albert Gu, Isys Johnson, Karan Goel, Khaled Saab, Tri Dao, Atri Rudra, and Christopher Ré. Combining recurrent, convolutional, and continuous-time models with linear state space layers. *Advances in neural information processing systems*, 34:572–585, 2021. 2

[15] Albert Gu, Karan Goel, and Christopher Ré. Efficiently modeling long sequences with structured state spaces. In *The International Conference on Learning Representations (ICLR)*, 2022. 2, 3

[16] Fengbin Guan, Xin Li, Zihao Yu, Yiting Lu, and Zhibo Chen. Q-mamba: On first exploration of vision mamba for image quality assessment. *arXiv preprint arXiv:2406.09546*, 2024. 2

[17] Ali Hatamizadeh and Jan Kautz. Mambavision: A hybrid mamba-transformer vision backbone. *arXiv preprint arXiv:2407.08083*, 2024. 2, 4

[18] Dailan He, Yaoyan Zheng, Baocheng Sun, Yan Wang, and Hongwei Qin. Checkerboard context model for efficient learned image compression. In *Proceedings of the IEEE/CVF Conference on Computer Vision and Pattern Recognition*, pages 14771–14780, 2021. 2, 4, 5

[19] Dailan He, Ziming Yang, Weikun Peng, Rui Ma, Hongwei Qin, and Yan Wang. Elic: Efficient learned image compression with unevenly grouped space-channel contextual adaptive coding. In *Proceedings of the IEEE/CVF Conference on Computer Vision and Pattern Recognition*, pages 5718–5727, 2022. 1, 2, 4, 5, 6, 7

[20] Kaiming He, Xiangyu Zhang, Shaoqing Ren, and Jian Sun. Deep residual learning for image recognition. In *Proceedings of the IEEE conference on computer vision and pattern recognition*, pages 770–778, 2016. 1

[21] Tao Huang, Xiaohuan Pei, Shan You, Fei Wang, Chen Qian, and Chang Xu. Localmamba: Visual state space model with windowed selective scan. *arXiv preprint arXiv:2403.09338*, 2024. 2

[22] Wei Jiang and Ronggang Wang. Mlic++: Linear complexity multi-reference entropy modeling for learned image compression. In *ICML 2023 Workshop Neural Compression: From Information Theory to Applications*, 2023. 1, 2, 5

[23] Jacob Devlin, Ming-Wei Chang, Kenton Lee, and Kristina Toutanova. Bert: Pre-training of deep bidirectional transformers for language understanding. In *Proceedings of naacl-HLT*, page 2. Minneapolis, Minnesota, 2019. 1

[24] Eastman Kodak. Kodak lossless true color image suite. <http://r0k.us/graphics/kodak>, 1993. 5

[25] A Burakhan Koyuncu, Han Gao, Atanas Boev, Georgii Gaikov, Elena Alshina, and Eckehard Steinbach. Contextformer: A transformer with spatio-channel attention for context modeling in learned image compression. In *European Conference on Computer Vision*, pages 447–463. Springer, 2022. 1, 3, 5, 6, 7

[26] Jinming Liu, Heming Sun, and Jiro Katto. Learned image compression with mixed transformer-cnn architectures. In *Proceedings of the IEEE/CVF conference on computer vision and pattern recognition*, pages 14388–14397, 2023. 1, 2, 5, 6

[27] Yue Liu, Yunjie Tian, Yuzhong Zhao, Hongtian Yu, Lingxi Xie, Yaowei Wang, Qixiang Ye, and Yunfan Liu. Vmamba: Visual state space model. *arXiv preprint arXiv:2401.10166*, 2024. 2

[28] Ming Lu, Peiyao Guo, Huiqing Shi, Chunlong Cao, and Zhan Ma. Transformer-based image compression. In

2022 Data Compression Conference (DCC), pages 469–469. IEEE, 2022. 2

[29] Harsh Mehta, Ankit Gupta, Ashok Cutkosky, and Behnam Neyshabur. Long range language modeling via gated state spaces. In *International Conference on Learning Representations*, 2023. 2

[30] David Minnen and Saurabh Singh. Channel-wise autoregressive entropy models for learned image compression. In *2020 IEEE International Conference on Image Processing (ICIP)*, pages 3339–3343. IEEE, 2020. 2, 4

[31] David Minnen, Johannes Ballé, and George D. Toderici. Joint autoregressive and hierarchical priors for learned image compression. *Advances in neural information processing systems*, 31, 2018. 2, 4

[32] Bo Peng, Eric Alcaide, Quentin Gregory Anthony, Alon Albalak, Samuel Arcadinho, Stella Biderman, Huanqi Cao, Xin Cheng, Michael Nguyen Chung, Leon Derczynski, et al. Rwkv: Reinventing rnns for the transformer era. In *The 2023 Conference on Empirical Methods in Natural Language Processing*, 2023. 1

[33] William B. Pennebaker and Joan L. Mitchell. *JPEG: Still image data compression standard*. Springer Science & Business Media, 1992. 1

[34] Yichen Qian, Xiuyu Sun, Ming Lin, Zhiyu Tan, and Rong Jin. Entroformer: A transformer-based entropy model for learned image compression. 2022. 1, 2, 3, 5

[35] Shiyu Qin, Jinpeng Wang, Yimin Zhou, Bin Chen, Tianci Luo, Baoyi An, Tao Dai, Shutao Xia, and Yaowei Wang. Mambavc: Learned visual compression with selective state spaces. *arXiv preprint arXiv:2405.15413*, 2024. 1, 2, 5, 6, 7

[36] Yihua Shao, Deyang Lin, Fanhu Zeng, Minxi Yan, Muyang Zhang, Siyu Chen, Yuxuan Fan, Ziyang Yan, Haozhe Wang, Jingcai Guo, Yan Wang, Haotong Qin, and Hao Tang. Trdq: Time-rotation diffusion quantization. *arXiv preprint arXiv:2503.06564*, 2025. 2

[37] Yuan Shi, Bin Xia, Xiaoyu Jin, Xing Wang, Tianyu Zhao, Xin Xia, Xuefeng Xiao, and Wenming Yang. Vmambair: Visual state space model for image restoration. *arXiv preprint arXiv:2403.11423*, 2024. 2

[38] Jimmy TH Smith, Andrew Warrington, and Scott Linderman. Simplified state space layers for sequence modeling. In *The Eleventh International Conference on Learning Representations*, 2022. 2

[39] Yu Sun, Xinhao Li, Karan Dalal, Jiarui Xu, Arjun Vikram, Genghan Zhang, Yann Dubois, Xinlei Chen, Xiaolong Wang, Sanmi Koyejo, et al. Learning to (learn at test time): Rnns with expressive hidden states. *arXiv preprint arXiv:2407.04620*, 2024. 1

[40] Mingxing Tan and Quoc Le. Efficientnet: Rethinking model scaling for convolutional neural networks. In *International conference on machine learning*, pages 6105–6114. PMLR, 2019. 1

[41] George Toderici, Wenzhe Shi, Radu Timofte, Lucas Theis, Johannes Balle, Eirikur Agustsson, Nick Johnston, and Fabian Mentzer. Workshop and challenge on learned image compression (clic2020). In *CVPR*, 2020. 5

[42] Ashish Vaswani, Noam Shazeer, Niki Parmar, Jakob Uszkoreit, Llion Jones, Aidan N Gomez, Łukasz Kaiser, and Illia Polosukhin. Attention is all you need. *Advances in neural information processing systems*, 30, 2017. 2

[43] Xinjian Wu, Fanhu Zeng, Xiudong Wang, and Xinghao Chen. Ppt: Token pruning and pooling for efficient vision transformers. *arXiv preprint arXiv:2310.01812*, 2023. 2

[44] Yijun Yang, Zhaohu Xing, and Lei Zhu. Vivim: a video vision mamba for medical video object segmentation. *arXiv preprint arXiv:2401.14168*, 2024. 2

[45] Peter Young, Alice Lai, Micah Hodosh, and Julia Hockenmaier. From image descriptions to visual denotations: New similarity metrics for semantic inference over event descriptions. *TACL*, 2:67–78, 2014. 5

[46] Fanhu Zeng and Deli Yu. M2m-tag: Training-free many-to-many token aggregation for vision transformer acceleration. In *Workshop on Machine Learning and Compression, NeurIPS 2024*, 2024. 2

[47] Lianghui Zhu, Bencheng Liao, Qian Zhang, Xinlong Wang, Wenyu Liu, and Xinggang Wang. Vision mamba: Efficient visual representation learning with bidirectional state space model. In *Forty-first International Conference on Machine Learning*, 2024. 2, 4

[48] Yinhao Zhu, Yang Yang, and Taco Cohen. Transformer-based transform coding. In *International Conference on Learning Representations*, 2022. 3

[49] Renjie Zou, Chunfeng Song, and Zhaoxiang Zhang. The devil is in the details: Window-based attention for image compression. In *Proceedings of the IEEE/CVF conference on computer vision and pattern recognition*, pages 17492–17501, 2022. 2

MambaIC: State Space Models for High-Performance Learned Image Compression

Supplementary Material

In the appendix, we provide details about evaluation metrics (Appendix A), datasets (Appendix B) and experimental settings (Appendix C). We also carry out more experimental results (Appendix D) and visualizations (Appendix E) to showcase the effectiveness of the proposed method qualitatively and quantitatively.

A. Explanation of Evaluation Metrics

PSNR. Peak Signal-to-Noise Ratio (PSNR) is a widely used metric to measure the quality of reconstructed images compared to the original images. It quantifies how much the noise (*i.e.*, distortion) has affected the quality of the image. Higher PSNR values typically indicate better quality, with less distortion or degradation in the image. In the main results, we convert PSNR into a logarithmic decibel unit for a better comparison.

MS-SSIM. Multiscale Structural Similarity Index (MS-SSIM) is an extension of SSIM (Structural Similarity Index). Concretely, SSIM evaluates the perceived quality of an image based on three main factors: luminance, contrast, and structure. The combination of these three components gives a measure of image quality that aligns more closely with human perception. Furthermore, MS-SSIM improves upon the original metric by evaluating similarity at multiple scales (resolutions) to better simulate human perception. In practical calculations, MS-SSIM combines the SSIM values from different scales using a weighted average.

B. Details about Evaluation datasets

Kodak. kodak is made up of 24 high-quality color images, each of them with 768×512 pixels. These images contains a diverse set of scenes, including landscapes, portraits, indoor settings, and textures, making the dataset representative of real-world visual content.

Tecnick. Tecnick consists of 100 images with 1200×1200 pixels. It is significant in evaluating image compression performance on numerous images with medium resolution.

CLIC Professional Valid. CLIC Professional Valid is a collection of images with 2K resolution proposed by the Third Challenge on Learned Image Compression. It validates the effectiveness of learned image compression approaches on high-resolution scenarios.

C. More Explanation of Experimental Settings

Detailed structure of channel-spatial context model is shown in Table A1. In the main paper, structure of hyper

encoder/decoder are a stack of convolution/deconvolution, VSS block and convolution/deconvolution. The convolution in spatial and channel entropy modeling Φ and Ψ_k holds $\text{kernel}=3$, $\text{stride}=2$ by default. In training procedure, the images are randomly cropped to 256×256 . We use Adam optimizer with $\beta_1 = 0.9$, $\beta_2 = 0.999$. The learning rate is set to $1e-4$ by default. During evaluation, the image is padded to fit for the compression and all evaluations are conducted on NVIDIA A100 under the same condition.

Table A1. Detailed architecture of channel-spatial context model.

Spatial context model Φ	Channel context model Ψ_k
in channel: M/K (spatial, $K = 5$)	in channel: k^*M/K (k^{th} , channel $k = 1, \dots, K$)
VSS block Conv 3×3 , s1, $2^*M/K$	VSS block Conv 3×3 , s1, $2^*M/K$
WLA module with channel-spatial aggregation	
fixed channel: $2^*M/K+2^*M/K+2^*M$ (spatial+channel+hyper) spatial reshape	
partition window size w Local Attention reverse window size w	

D. More Experimental Results

Effectiveness of SSM block in different modules. We apply SSM block as foundation block in both nonlinear transform and context model. To figure out the utility of different foundation blocks in each modules, we additional conduct experiments and comprehensively compare the results with different variants of model that is equipped with nonlinear transform/context model of CNN/Transformer/SMM structure. Results in Table A2 reveals that the structure of main transform, *i.e.*, encoder/decoder, also influences the performance and further demonstrates the effectiveness of the proposed structure incorporating SSM blocks.

E. More Attention Map Comparison

Corresponding to visualization results in the main paper, we showcase more comparison of attention map as opposed to models w/o context entropy model and w/o window-based local attention in Figure A1 and Figure A2 to further verify the effectiveness of each proposed component in MambaIC.

Table A2. Different variants of nonlinear transform architecture.

Main Transform	Hyper Transform	Context Model	Decoding Latency (ms)	BD-Rate
CNN	CNN		35.53	-3.81%
	Transformer		-	-
	State Space Model		35.64	-7.15%
Transformer	CNN		-	-
	Transformer		48.74	-7.19%
	State Space Model		37.82	-9.30%
State Space Model	CNN		-	-
	Transformer		-	-
	State Space Model		39.42	-12.52%

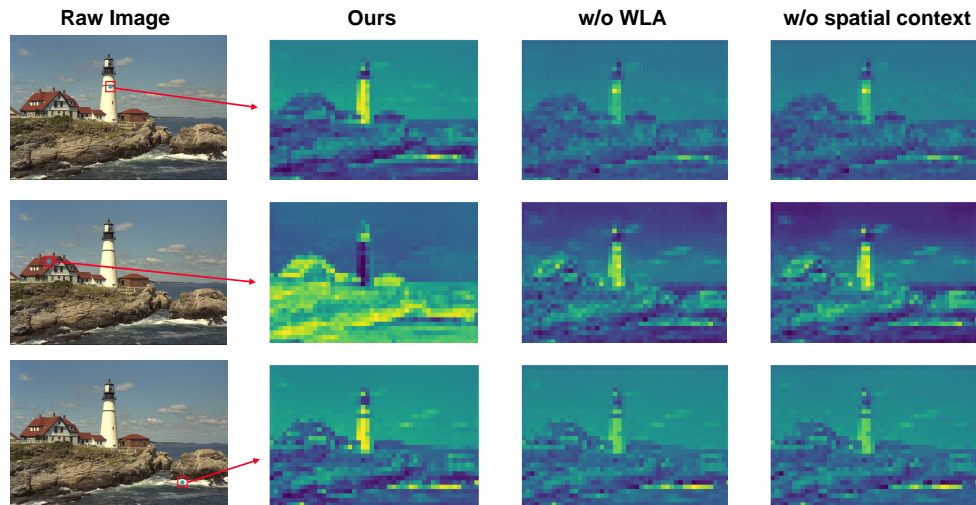


Figure A1. Attention maps of latent representations y of *kodim21.png* in Kodak.

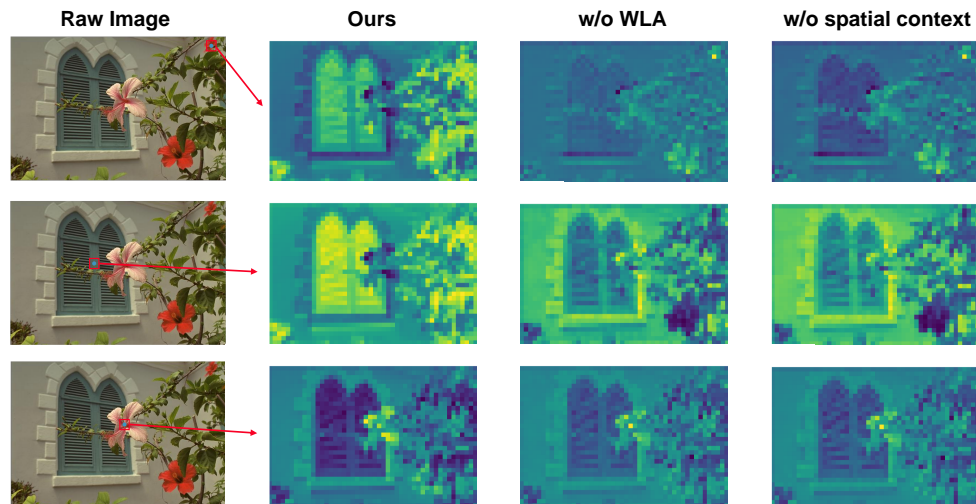


Figure A2. Attention maps of latent representations y of *kodim07.png* in Kodak.